








Differential environmental and genomic architectures shape the natural diversity for trichome patterning and morphology in different *Arabidopsis* organs

Noelia Arteaga¹  | Belén Méndez-Vigo¹  | Alberto Fuster-Pons¹  |
 Marija Savic¹  | Alba Murillo-Sánchez¹  | F. Xavier Picó²  |
 Carlos Alonso-Blanco¹ 

¹Departamento de Genética Molecular de Plantas, Centro Nacional de Biotecnología (CNB), Consejo Superior de Investigaciones Científicas (CSIC), Madrid, Spain

²Departamento de Ecología Integrativa, Estación Biológica de Doñana (EBD), Consejo Superior de Investigaciones Científicas (CSIC), Sevilla, Spain

Correspondence

Carlos Alonso-Blanco, Genética Molecular de Plantas, Centro Nacional de Biotecnología (CNB), Consejo Superior de Investigaciones Científicas (CSIC), C/Darwin 3, Cantoblanco, Madrid 28049, Spain.
 Email: calonso@cnb.csic.es

Funding information

Ministerio de Ciencia e Innovación (MCIN); Agencia Estatal de Investigación (AEI)

Abstract

Despite the adaptive and taxonomic relevance of the natural diversity for trichome patterning and morphology, the molecular and evolutionary mechanisms underlying these traits remain mostly unknown, particularly in organs other than leaves. In this study, we address the ecological, genetic and molecular bases of the natural variation for trichome patterning and branching in multiple organs of *Arabidopsis* (*Arabidopsis thaliana*). To this end, we characterized a collection of 191 accessions and carried out environmental and genome-wide association (GWA) analyses. Trichome amount in different organs correlated negatively with precipitation in distinct seasons, thus suggesting a precise fit between trichome patterning and climate throughout the *Arabidopsis* life cycle. In addition, GWA analyses showed small overlapping between the genes associated with different organs, indicating partly independent genetic bases for vegetative and reproductive phases. These analyses identified a complex locus on chromosome 2, where two adjacent MYB genes (*ETC2* and *TCL1*) displayed differential effects on trichome patterning in several organs. Furthermore, analyses of transgenic lines carrying different natural alleles demonstrated that *TCL1* accounts for the variation for trichome patterning in all organs, and for stem trichome branching. By contrast, two other MYB genes (*TRY* and *GL1*), mainly showed effects on trichome patterning or branching, respectively.

KEYWORDS

Arabidopsis thaliana, climate, Genome-Wide Association (GWA), *GLABRA1* (*GL1*), precipitation, trichome branching, trichome patterning, *TRICHOMELESS 1* (*TCL1*), *TRIPTYCHON* (*TRY*)

This is an open access article under the terms of the Creative Commons Attribution-NonCommercial-NoDerivs License, which permits use and distribution in any medium, provided the original work is properly cited, the use is non-commercial and no modifications or adaptations are made.

© 2022 The Authors. *Plant, Cell & Environment* published by John Wiley & Sons Ltd.

1 | INTRODUCTION

Trichomes, or plant hairs, are highly differentiated epidermal cells that outgrow from plant aerial surfaces, to closely interact with the surrounding environment. They have been shown to protect from sunlight and heat, hence providing adaptations to draught and UV radiation (Bickford, 2016; Hauser, 2014). In addition, trichomes provide active physical and chemical barriers against herbivore insects, thus becoming a developmental mechanism for plant defense (Dalin et al., 2008; Fürstenberg-Hägg et al., 2013; Zhou et al., 2017).

Trichomes are present in most Angiosperms, but the morphology, as well as the amount and distribution (trichome patterning) in different organs, are highly variable among species. Most plants develop trichomes in leaves, although they can also be formed in any aerial organ, including all floral whorls (Judd et al., 1999). Trichomes can also vary from uni- to multicellular structures, from simple (unbranched) to highly branched, and can be glandular or not (Balkunde et al., 2010; Chalvin et al., 2020; Z. Wang, Yang, et al., 2019). Owing to the broad interspecific diversity existing for trichome patterning and morphology, these features have been classically used as plant taxonomic characters (Judd et al., 1999; Tutin et al., 1993). However, trichome patterning also shows substantial genetic and environmental intraspecific variation. On one hand, individuals from natural populations may differ largely in the density of trichomes in particular organs, which is presumed to reflect adaptations to their local environments (Hauser, 2014). On the other hand, trichome density is a highly plastic trait, and wide genetic intraspecific variation has been described in response to multiple environmental factors, including herbivores, light or water stress (Hahn et al., 2019; Kooyers et al., 2015; Mediavilla et al., 2019; Züst et al., 2012).

In the past two decades, the genetic and molecular bases of trichome development have been elucidated, mainly in the wild model plant *Arabidopsis* (Balkunde et al., 2010; Marks, 1997; Pattanaik et al., 2014). This species has been characterized as having unicellular trichomes, which are branched in leaves, simple and branched in basal stem internodes and simple in sepals. In addition, the upper stem internodes, pedicels and fruits of *Arabidopsis* have been described as glabrous (Al-Shehbaz & O'Kane, 2002; Hülskamp & Schnittger, 1998), but it has been recently shown that this is not always the case (Arteaga et al., 2021). Analyses of *Arabidopsis* artificially induced mutants have identified ~140 different genes regulating the main two phases of trichome development and its hormonal and environmental interactions (Dai et al., 2010; Pattanaik et al., 2014). Leaf trichome patterning is first established by a well-known gene network regulating trichome cell initiation, which involves a trimeric activating complex encoded by *GLABRA1* (*GL1*), *GLABRA3/ENHANCER OF GLABRA3* (*EGL3*) and *TRANSPARENT TESTA GLABRA1* (*TTG*). This complex promotes trichome initiation by activating the expression of the homeodomain gene *GLABRA2* (*GL2*). In addition seven genes encoding single repeat R3 MYB transcription factors repress trichome initiation by disrupting the function of the trimeric complex (Wang & Chen, 2014). Subsequently,

trichome branching is regulated by genes involved in the maintenance of trichome cell fate, as well as in the regulation of mitosis and endoreduplication (Balkunde et al., 2010; Fambrini & Pugliesi, 2019). Several genes, however, such as *TRIPTYCHON* (*TRY*), show pleiotropic effects on both developmental steps, trichome patterning and branching, which reveals intricate interactions in this regulatory network (Folkers et al., 1997; Schellmann et al., 2002; Schnittger et al., 1998).

Although most mutant analyses have been carried out in leaves, several studies have identified several genes encoding C2H2 zinc finger transcription factors involved in trichome development specifically in stems and pedicels (Pattanaik et al., 2014; Sun et al., 2015). In addition, leaf trichome patterning is an age-dependent developmental process that is regulated by microRNA 156 (*miR156*), *miR172* and other regulatory genes, which also affect the transition from juvenile to adult leaf stages, and from vegetative to reproductive phases (Aguilar-Jaramillo et al., 2019; Wang, Zhou, et al., 2019). These genes are further regulated by hormones, including gibberellins, cytokinins or jasmonic acid, thus providing the mechanisms to integrate environmental signals in the regulation of trichome development (Fambrini & Pugliesi, 2019). Currently, numerous studies are also dissecting the molecular mechanisms regulating trichome formation in crop plants with multicellular, glandular or fibre-like trichomes, such as cucumber, tomato or cotton (reviewed in Chalvin et al., 2020; Liu et al., 2016; Schuurink & Tissier, 2020; Wang, Yang, et al., 2019). Hence, a high functional conservation in trichome formation has been revealed for several MYB, C2H2 zinc finger and homeodomain proteins, across Angiosperms.

In contrast to the successful efforts to disentangle the molecular mechanisms underlying trichome development (Chalvin et al., 2020; Pattanaik et al., 2014), only a handful of genes have been identified accounting for the intraspecific diversity for trichome patterning, whereas the natural variation for trichome branching has not been approached (Hauser, 2014). Current studies have been mostly focused on leaf trichomes and have shown that loss-of-function mutations of *GL1*, encoding an R2R3 MYB transcription factor, cause a qualitative glabrous phenotype segregating in numerous species (Bloomer et al., 2012; Hauser et al., 2001; Kivimäki et al., 2007; Li et al., 2013). In addition, *ATMYC1* and *ENHANCER OF TRY AND CPC* (*ETC2*) in *Arabidopsis*, and *Hairy* in *Antirrhinum* species, contribute to the quantitative variation for leaf trichome density (Hilscher et al., 2009; Symonds et al., 2011; Tan et al., 2020). Furthermore, the molecular bases of *Arabidopsis* natural variation for trichome patterning in other organs have been also recently pursued through the analysis of a genetic lineage from the Iberian Peninsula developing trichomes in fruits and pedicels (Arteaga et al., 2021). Thus, it has been shown that a gain-of-function allele of *GL1*, and partial loss-of-function alleles of *TRICHOMELESS 1* (*TCL1*) and *TRY* interact synergistically to trigger such *Arabidopsis* trichome patterning innovation evolved exclusively in this geographic region.

In this study, we have addressed the ecological, genetic and molecular bases of the natural variation for trichome patterning and

branching in multiple organs of *Arabidopsis*, including leaves, different sections of stems and pedicels. To achieve these goals, we have analysed a regional collection of 191 wild accessions from the Iberian Peninsula, which encompasses genomic and environmental information (1001 Genomes Consortium, 2016; Manzano-Piedras et al., 2014). Previous analyses of several traits (Arteaga et al., 2021; Tabas-Madrid et al., 2018) have shown that Iberia harbours the largest *Arabidopsis* diversity in Eurasia, a consequence of its double colonization from Africa and Europe (1001 Genomes Consortium, 2016; Durvasula et al., 2017). We have now phenotypically characterized this resource for trichome patterning in multiple organs, and have used these phenotypes for two kinds of analyses. First, we have analysed the relationship between climate and trichome patterning. Second, we have carried out a comparative genome-wide association (GWA) study of trichome patterning in vegetative and reproductive phases. In addition, we have characterized transgenic lines carrying different natural alleles of three candidate genes, *TCL1*, *TRY* and *GL1*, for their effects on trichome patterning and branching. From these analyses, we concluded that (i) the diversity for trichome patterning across *Arabidopsis* life cycle shows a complex pattern of adaptation, where the climate is likely a major adaptive factor; (ii) different genomic architectures underlie *Arabidopsis* natural variation for trichome patterning in vegetative and reproductive organs; and (iii) *TCL1*, *TRY* and *GL1* contribute differentially to the natural variation for trichome patterning and branching in several organs.

2 | MATERIALS AND METHODS

2.1 | Plant material

A previously described collection of 191 genetically distinct wild accessions of *Arabidopsis* from the Iberian Peninsula was analysed (Arteaga et al., 2021; Castilla et al., 2020; Tabas-Madrid et al., 2018) (Supporting Information: Table S1). These accessions are publicly available through Nottingham *Arabidopsis* Stock Centre (NASC; <http://arabidopsis.info>).

A set of 22 introgression lines previously developed from the Iberian accession Don-0 and the *Ler* reference strain were analysed (Arteaga et al., 2021). These lines carry Don-0 alleles of *MAU2/TCL1*, *MAU3/GL1* or *MAU5/TRY*, in a *Ler* genetic background. They correspond to three independent lines for each of the seven different combinations of one to three *MAU* genomic regions from Don-0, and are named as IL followed by the numbers of the *MAU* loci carrying Don-0 alleles (IL-2, IL-3, IL-5, IL-23, IL-25, IL-35 and IL-235). An additional line IL-1235 carrying Don-0 alleles in *MAU1*, *MAU2*, *MAU3* and *MAU5* was also included.

The *gl1-1* spontaneous mutant (N1688), and the T-DNA insertion mutants *tc1* (N675198) and *try* (N6518), all in the *Col* background, have been previously described (Arteaga et al., 2021).

A set of 134 T₃ independent transgenic lines homozygous for genomic constructs of *TCL1*, *TRY* or *GL1*, previously developed and

analysed for trichome patterning in fruits (Arteaga et al., 2021), were characterized for trichome traits in leaves and stems. In brief, transgenic lines included six genomic constructs derived from Don-0 and *Ler* accessions, with sizes of 3.8, 6.7 and 5.1 kb for *TCL1*, *TRY* and *GL1*, respectively. These constructs comprised the following genomic regions: 2.0, 3.9 and 1.7 kb of promoter and 5'-UTR; 1.2, 1.0 and 1.5 of coding sequences; and 0.6, 1.8 and 1.9 kb of the 3' regions of each gene, respectively. Two additional *TCL1* transgenes were present in these lines, which corresponded to chimeric genomic constructs with the promoter, 5'-UTR and the first coding exon of *TCL1* from Don-0 or *Ler*, but the remaining coding sequence and the 3' region from *Ler* or Don-0, respectively. Transgenic lines were developed in the following genetic backgrounds: the mutant *tc1* and line IL-235 for the four *TCL1* constructs; *try* mutant, as well as the lines IL-235 and IL-1235, for the two *TRY* genomic constructs; the mutant line *gl1* for the two *GL1* genomic constructs.

2.2 | Growth conditions and phenotypic analyses

Plants were grown in pots with soil and vermiculite at 3:1 proportion using growth chambers set up at 21°C and a long-day (LD; 16 h of cool-white fluorescent light, photon flux of 100 $\mu\text{mol}/\text{m}^2\text{s}$) or a short-day (SD; 8 h of cool-white fluorescent light, photon flux of 100 $\mu\text{mol}/\text{m}^2\text{s}$) photoperiod. Vernalization treatment was given in a cold chamber at 4°C, with SD photoperiod, during 8 weeks.

For phenotypic characterization, all accessions, ILs or transgenic lines carrying transgenes of the same gene, were analysed simultaneously in the same experiment. We used two (accessions), or three (ILs and transgenic lines) complete blocks designs with randomization, each block containing one pot with six plants per line. Given the large variation among Iberian accessions for flowering time (Tabas-Madrid et al., 2018), accessions were grown under SD photoperiod during 2 months, which avoided flowering induction in most of them. After leaf sampling, flowering initiation was induced by giving a vernalization treatment. Pots were then moved to a growth chamber with LD photoperiod for measurements of trichome patterning in the main inflorescence. Since ILs and transgenic lines were early flowering, they were characterized under LD photoperiod without vernalization treatment.

Trichome patterning was measured in leaves, stems and fruit pedicels by recording two quantitative traits, leaf trichome density (LTD) and stem trichome pattern (STP), as well as two qualitative traits, binary stem trichome pattern (STPb) and binary pedicel trichome pattern (PTPb). LTD was quantified as the ratio between the number of trichomes in the adaxial side of leaf number 14–16 (for accessions, grown under SD photoperiod), or 5–6 (for ILs and transgenic lines, grown under LD photoperiod) and leaf surface in square millimeters. Leaves were collected and photographed when they were fully expanded, and leaf trichome numbers and surfaces were scored on the photographs using the image analysis software ImageJ (<http://imagej.net>). Trichome density in the stem of the main inflorescence follows an acropetal reduction, with the lowest

internodes between cauline leaves showing the highest density. Therefore, STP was quantified as the number of internodes between cauline leaves, or the first fruits, developing trichomes. For the characterization of introgression and transgenic lines, STP was quantified up to the first 35 internodes. However, given the large amount of natural variation for the number of cauline leaves, only the first eight internodes were considered for STP in the characterization of accessions. In addition, we recorded the overall trichome patterning in the upper segment of the main stem, which develops fruits instead of cauline leaves, as the qualitative trait STPb. For that, plants were classified according to the presence or absence of trichomes in the internodes between, at least, the first five fruits. Finally, trichome patterning in fruit pedicels was also scored as the qualitative measurement PTPb, by classifying plants for the absence or presence of trichomes in the pedicels of all first five fruits or more. The latter was scored to enable comparisons of trichome pattern variation in leaves and stems with that previously described in fruits and pedicels (Arteaga et al., 2021).

Trichome branching was quantified in the basal internodes of the main stem. We chose this organ because stem trichomes show an overall reduction in branch number following an acropetal fashion, Col and Ler reference strains displaying mainly simple trichomes in these internodes (Hülkamp & Schnitter, 1998). Trichome branching was quantified as the proportion of trichomes with one (simple), two or more than two branches in the two cm up and down from the first or second node, for genotypes in Ler and Col genetic background, respectively. Stems were collected and photographed when plants were fruiting, which ensured they were fully elongated, and the number of trichomes with different number of branches were recorded using the cell counter tool of the software ImageJ (<http://imagej.net>).

2.3 | Genetic and GWA analyses

GWA analyses were carried out using the mean values of all plants phenotyped for each accession and the SNP data set previously developed from the genome sequences of 235 Iberian accessions (Arteaga et al., 2021). These SNPs were filtered to keep those segregating in the 184 non-glabrous accessions, with a minor allele frequency of five accessions ($MAF \geq 3\%$). Thereby we used 1 710 184 informative SNPs, including 306 632 with no missing data, and an average missing frequency of 8.9%. These SNPs were located in 31 984 genes out of the 32 833 annotated open reading frames in TAIR10 (97.4%), and all but 97 genes contained more than one SNP. This corresponded to an average of 53 informative SNPs per gene, and one SNP every 73 bp on the genomes of the 184 Iberian accessions.

GWA analyses were carried out using the standard mixed linear model implemented in Tassel v.5 (Bradbury et al., 2007). The genetic kinship matrix included as covariate to control for population structure was estimated from the proportion of shared alleles (Atwell et al., 2010). A high significance threshold of $-\log(P) = 7.53$,

corresponding to 5% with Bonferroni correction for multiple tests, was applied to detect the most significant associations. In addition, we also applied a low significance threshold of $-\log(P) = 4$ to detect potential associations, as described for large SNP datasets (Frachon et al., 2017; Togninalli et al., 2017). Given the complexity of these quantitative traits and the limited population size, comparisons of GWA results among traits are based on the overlapping of genes instead of SNPs. Associated genes detected by GWA analyses were derived from TAIR10 gene locations of significant SNPs, but including the two flanking genes when SNPs were located in intergenic regions.

For each trait, the phenotypic variance was partitioned into variances attributed to genotype (V_G , accession effect) and error (V_E) using a Type III random effect analysis of variance (ANOVA) for the model $y = \mu + G + E$. Variance components were used to estimate broad-sense heritabilities (h^2_b) according to the formula $h^2_b = V_G / (V_G + V_E)$ where V_G is the among-genotypes (accessions) variance component and V_E is the residual variance. Genetic correlations between different traits were estimated as $r_G = \text{COV}_{1,2} / \sqrt{(V_{G1} \times V_{G2})}$, where $\text{COV}_{1,2}$ is the covariance of trait means, and V_{G1} and V_{G2} are the among-genotypes variance components for those traits (Keurentjes et al., 2007). Significances of genetic correlations were estimated by permutations (McKay et al., 2003). Similarly, heritabilities of trichome variables explained by associated SNPs were estimated as variance components derived from Type III ANOVAs including SNPs as explanatory factors. ANOVAs and variance component analyses were estimated using the general linear models (GLMs) implemented in SPSS software v.27. The heritability of trichome variables explained by the kinship matrix was estimated by genomic best linear unbiased prediction (BLUP) as implemented in Tassel v.5 (Bradbury et al., 2007).

To find known genes involved in trichome patterning and development that are associated with phenotypic variables, we generated a list of 140 candidate genes (Supporting Information: - Table S4). This list compiled the genes reported in the TrichOME database (Dai et al., 2010) and previous reviews (Doroshkov et al., 2019; Pattanaik et al., 2014; Wang & Chen, 2014). Enrichment of these known trichome genes among the SNPs significantly associated with phenotypic variables was estimated by permutations as previously described (Brachi et al., 2010), using an R script kindly provided by Fabrice Roux (CNRS, Toulouse, France). Enrichment was calculated as the ratio between the number of top associated SNPs within known trichome genes (± 10 kb) and the average number of the null distribution.

2.4 | Environmental analyses

The spatial autocorrelation of trichome pattern variables was analysed using correlograms generated with the software PASSaGE v.2 (Rosenberg & Anderson, 2011). For each variable, Moran's I autocorrelation coefficients were calculated and plotted for 15 successive spatial intervals, coefficients ranging between 1 (positive spatial autocorrelation) and -1 (negative spatial autocorrelation).

Significances of Moran's I values were calculated from 1000 permutations.

A total of 79 climatic variables were obtained from a geographic information system previously developed for the Iberian collection of *Arabidopsis* accessions (Manzano-Piedras et al., 2014), which include 19 bioclimatic variables (Hijmans et al., 2005), as well as mean, maximum and minimum temperatures, total precipitation and mean solar radiation for each month. The relationships between climate variables and quantitative or binary traits were tested with simultaneous autoregressive models (SAR; Kissling & Carl, 2008) or autologistic regression models (Dormann, 2007), respectively. SAR is a multiple regression technique explicitly developed for spatial data, which uses generalized least squares to estimate regression parameters while including in the model an additional term for the autocorrelation matrix of the errors (Beale et al., 2010). Autologistic regression models include an autocovariate to correct for the effect of spatial autocorrelation of the response variable. The relationships between significant climatic variables and quantitative phenotypes were also tested by Geographically Weighted Regression (GWR), which perform a local regression test using an optimized bandwidth corresponding to the 10%–15% neighbour accessions. All spatial regression analyses were carried out using SAM software v.3.1 (Rangel et al., 2010). Glabrous accessions were not considered in these analyses.

2.5 | Gene sequencing and expression

For sequencing the *GL1* gene in the seven glabrous accessions, four overlapping fragments of 0.7–0.8 kb were polymerase chain reaction (PCR) amplified using oligonucleotides previously described (Arteaga et al., 2021) and products were sequenced using an ABI PRISM 3730xl DNA analyser. These gene sequence data have been submitted to the GenBank/EMBL databases under the accession numbers OK539781–OK539787.

For expression analyses, plants were grown as described for phenotypic analyses, but pots contained ~50 (for leaf samples) or 9 (for stems and flowers) plants. After sowing, pots were placed at 4°C and SD photoperiod for seed stratification during 4 days. Thereafter, pots were transferred to a growth chamber with LD photoperiod and 21°C. Genotypes to be compared (parental accessions, or transgenic lines with transgenes of the same gene) were grown simultaneously in a single experiment, including three pots per genotype (or nine pots for controls), organized in three randomized blocks. For leaf samples, 14- to 18-day-old rosettes were harvested, whereas for flower samples, buds of the main inflorescences were collected 5 days after flowering initiation (30- to 40-day-old plants depending on the genetic background). For stem samples, the shoot of the main inflorescence was collected from the same plants used for flowers, after removing cauline leaves, lateral branches and flower buds. Tissue from the three blocks of each genotype was mixed before RNA isolation. *TCL1*, *TRY* and *GL1* expression was analysed by RT-quantitative PCR (RT-qPCR) as described in Arteaga et al. (2021).

Mean and standard errors were derived from three biological replicates (RNA isolated from plants grown in different pots) for parental accessions, or from three technical replicates (RT-qPCR wells from the same cDNA sample) for transgenic lines.

2.6 | Other statistical analyses

Phenotypic and gene expression differences between accessions and organs were tested by mixed GLMs including genotypes and organs as fixed effect factors and replicates as random effect factors. Differences between transgenic lines were also tested by mixed GLMs including transgenes as a fixed factor and lines (nested within transgenes) as random factor. In introgression lines, the additive and interaction effects of *TCL1/MAU2*, *GL1/MAU3* and *TRY/MAU5* loci were tested by GLMs including the three loci as fixed effect factors. These analyses were carried out with the statistical packages SPSS v.27 or Statistica v.8. All statistical analyses are detailed in Supporting Information: Table S3.

3 | RESULTS

3.1 | Natural variation for trichome patterning and branching in leaves, stems and pedicels

To quantify the diversity of trichome patterns in different organs across the vegetative and reproductive phases of *Arabidopsis*, we measured two quantitative and two qualitative traits in 191 wild accessions from the Iberian Peninsula (Figure 1). Leaf trichome density (LTD) showed substantial variation, including seven glabrous accessions collected in different natural populations (Figure 1a–c). Large quantitative variation was also found for stem trichome pattern (STP) measured as the number of stem internodes developing trichomes, which varied from the formation of trichomes only in the two basal internodes, up to the whole stem length. These two quantitative traits showed weak genetic correlation ($r_G = 0.26$; Figure 1b) indicating independent genetic bases for trichome pattern in both organs. In addition, analyses of the binary STP (STPb) and the binary pedicel trichome pattern (PTPb) identified 16 accessions (8.4%) with trichomes in fruiting stem internodes and pedicels (Figure 1b–d). Two other accessions also displayed trichomes in pedicels but not in the fruiting stems, in agreement with a strong genetic correlation between both traits ($r_G = 0.94$; $p < 0.001$). Consistently, binary traits showed moderate correlations with STP ($r_G = 0.60$ – 0.64 ; $p < 0.01$), but low with LTD ($r_G = 0.17$ – 0.20 ; $p < 0.01$).

Natural accessions also differed in trichome morphology in the various organs. Overall, trichomes in leaves, pedicels and upper internodes of stems, were mostly branched in all strains developing trichomes in these organs (Figure 1d). However, basal internodes of stems varied from combinations of simple (unbranched) and branched trichomes (Col and Ler laboratory strains) to the development of only simple or branched trichomes (e.g., Bra-0 and Don-0 in Figure 1d).

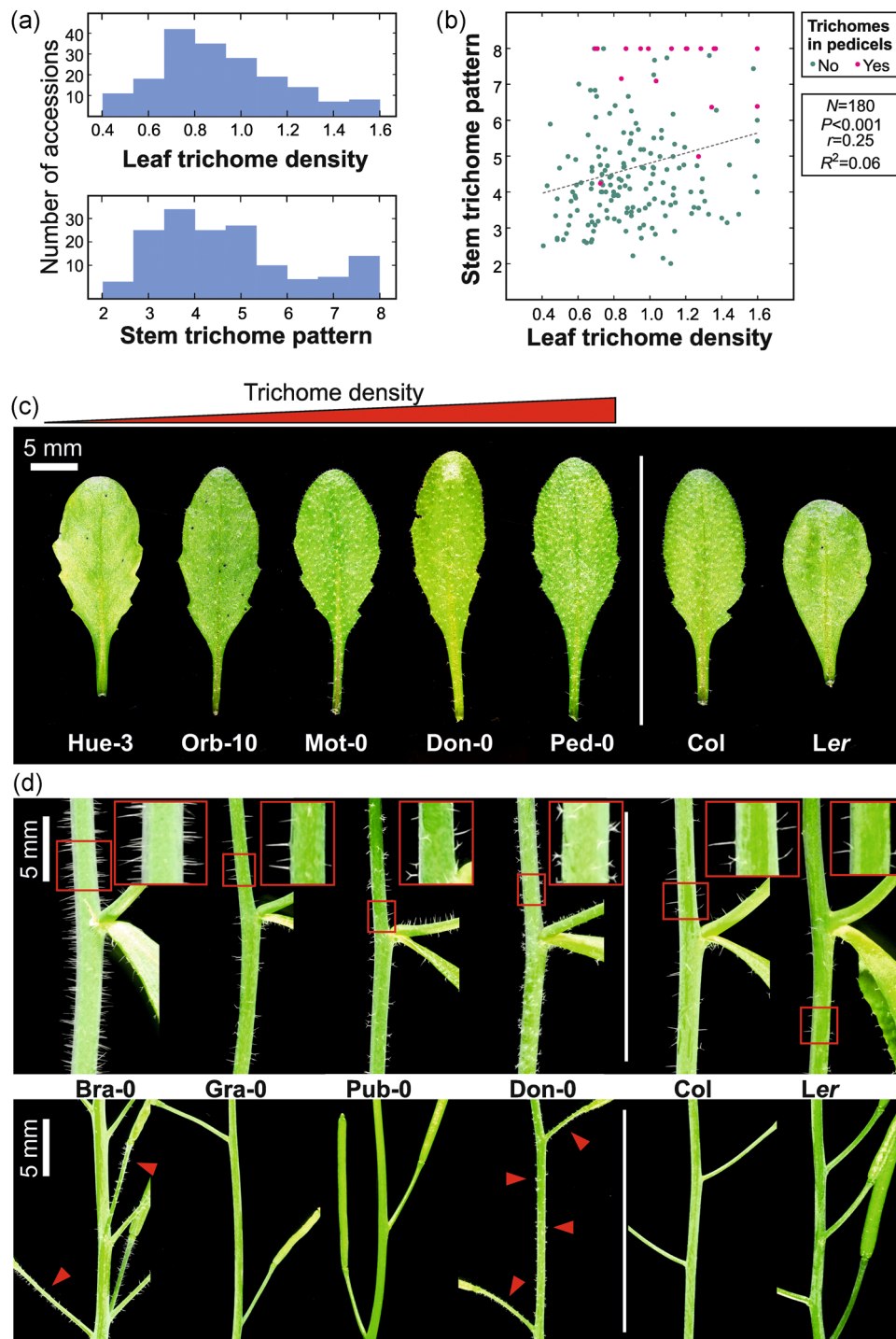


FIGURE 1 Natural variation for trichome patterning and branching in Arabidopsis. (a) Frequency distributions of leaf trichome density (number of trichomes per square millimeter) and stem trichome pattern (number of internodes with trichomes) in Iberian accessions. (b) Relationship between leaf trichome density and trichome pattern in stems and pedicels. Legend close to graph shows the Pearson correlation between accession mean values of leaf and stem trichome variables. In (a and b), glabrous accessions were not included. (c) Leaves of natural accessions with different trichome patterns, arranged from glabrous to high trichome density. (d) Variation for trichome patterning and branching in basal stem internodes (upper panel), as well as in upper stem internodes and fruit pedicels (lower panel). In the upper panel, insets show stem close-ups illustrating the diversity for trichome branching. In the lower panel, arrowheads point to trichomes in pedicels or fruiting stems. Leaves and stems of the reference strains Col and Ler are shown in the right side of each panel

3.2 | Geographic and climatic distribution of trichome pattern variation in different organs

The seven glabrous accessions occurred in populations spread throughout the Iberian Peninsula (Figure 2a,b). Sequencing of *GL1* in these strains identified one large (1123 bp) and two small (1 bp) deletions predicted to generate truncated proteins, and three missense mutations in highly conserved regions (Figure 2a). Hence, six independent loss-of-function mutations of the trichome promoter gene *GL1* encoding an R2R3 MYB transcription factor cause glabrousness in this geographic region. One of the truncations was found in two populations, Cam-6 and Cas-15, that are located 100 km apart, indicating a long spread of this loss-of-function mutation. In contrast to the glabrous phenotype, accessions developing trichomes in upper stem internodes were mostly distributed in Western Iberia, and absent in the northeast area of this region (Figure 2b). Seventy-five percent of these accessions belonged to the relict genetic group, which has been previously described as a highly differentiated lineage that split from the non-relict lineage before the last glaciations (1001 Genomes Consortium, 2016; Durvasula et al., 2017; Tabas-Madrid et al., 2018). This geographic and genetic distribution was similar to that previously described for accessions with trichomes in pedicels and fruits (Arteaga et al., 2021). On the contrary, all glabrous accessions corresponded to non-relict populations (Supporting Information: Table S1). Furthermore, spatial autocorrelation analyses only detected positive Moran's *I* values for leaf trichome density up to 72 km ($I=0.066$; $p=0.016$), thus indicating very restricted spatial structure for trichome traits (Supporting Information: Figure S1).

To identify environmental factors that might contribute to maintain the genetic diversity for trichome patterns in nature, we analysed the relationships between phenotypic traits and climatic factors at the local populations of origin. These analyses were carried out using autoregressive models, which take into account spatial autocorrelations (see Section 2), and included annual and monthly temperature, precipitation and solar radiation variables. All quantitative and qualitative trichome traits showed significant negative regressions with monthly precipitations, indicating that the lower the rain, the higher the trichome formation (Figure 2c). Nevertheless, only regressions with stem trichome variables were significant at $p < 0.0006$ (corresponding to 5% with Bonferroni correction for multiple testing). Overall, different traits showed maximum associations with different seasons of the year. LTD was associated mainly with fall and winter precipitation, STP with winter and spring, whereas trichomes in the upper stem and pedicels appeared correlated with spring and summer precipitations. Thereby, the trichome pattern of each organ seemed coupled with precipitation in the season at which it is phenologically developed in Iberian populations (Exposito-Alonso et al., 2018; Gomas et al., 2011). In addition, STP showed a significant positive correlation with solar radiation along the year (Figure 2c), further stressing a role of climate as driver of trichome pattern diversity.

We further explored the relationship between quantitative trichome traits and precipitation by carrying out Geographically Weighted Regressions, which estimate coefficients at each location using 10%–15% neighbouring populations. These analyses showed that regressions varied strongly across Iberia but displayed differential geographic patterns for leaves and stems (Figure 2d). The areas showing differential regressions between LTD and precipitation did not differ in mean precipitation ($p=0.22$), but showed variation for LTD (Figure 2d) because the northeastern locations displaying the strongest values had lower average trichome density ($p=0.002$), as tested by ANOVA tests. On the contrary, for STP, the maximum regression coefficients were detected in the northwestern area, which showed significantly higher precipitation ($p < 0.001$) but did not differ from other subregions in the average STP values ($p=0.74$). These results suggest that the strength of the relationship between the trichome trait and precipitation is conditioned by the particular range of the precipitation for STP, whereas it likely depends on the local interaction with other environmental factors for LTD. Therefore, although precipitation appears as the main climatic factor that presumably maintains trichome diversity in nature, additional local factors contribute to differentially shape the genetic variation affecting different organs.

3.3 | Genome-wide analyses of trichome patterning in leaves, stems and pedicels

To determine the genomic architecture underlying the natural variation for trichome patterning along plant development, we carried out GWA analyses using 1.7 million single nucleotide polymorphisms (SNPs) segregating in the 184 Iberian non-glabrous accessions (Figure 3). The two quantitative traits, LTD and STP, showed low correlation with the genomic background of the accessions, as measured by the phenotypic variance explained by a kinship matrix (Table 1). Despite this low correlation, only a single genomic region was detected on chromosome 2 for LTD and STP at $-\log(P) > 7.53$ (corresponding to 5% with Bonferroni correction for multiple testing; Figure 3b,c). At a lower statistical significance of $-\log(P) > 4$, a total of 178 and 650 SNPs appeared associated with LTD and STP, respectively, which affected to 78 and 356 genes. By contrast, the two binary traits, STPb and PTPb, displayed a stronger correlation with the genomic background, and a much higher number of SNPs and genes were detected for both traits at high statistical significance (Figure 3d,e and Table 1). Comparisons of results among the four traits (Table 1 and Figure 3a) showed that LTD only shared 1.1%–2.6% of the genes associated with stem or pedicel trichome patterns, in agreement with the low correlations between these traits. However, the latter traits shared between 18.1% and 64.1% of the genes detected in these analyses. Accordingly, comparison of the 10 top genomic regions detected for each trait (Supporting Information: Table S2) showed zero or one common genes between LTD and the remaining traits, whereas STP, STPb and PTPb shared two to six of the 10 top genes. Analysis of 140 known genes involved

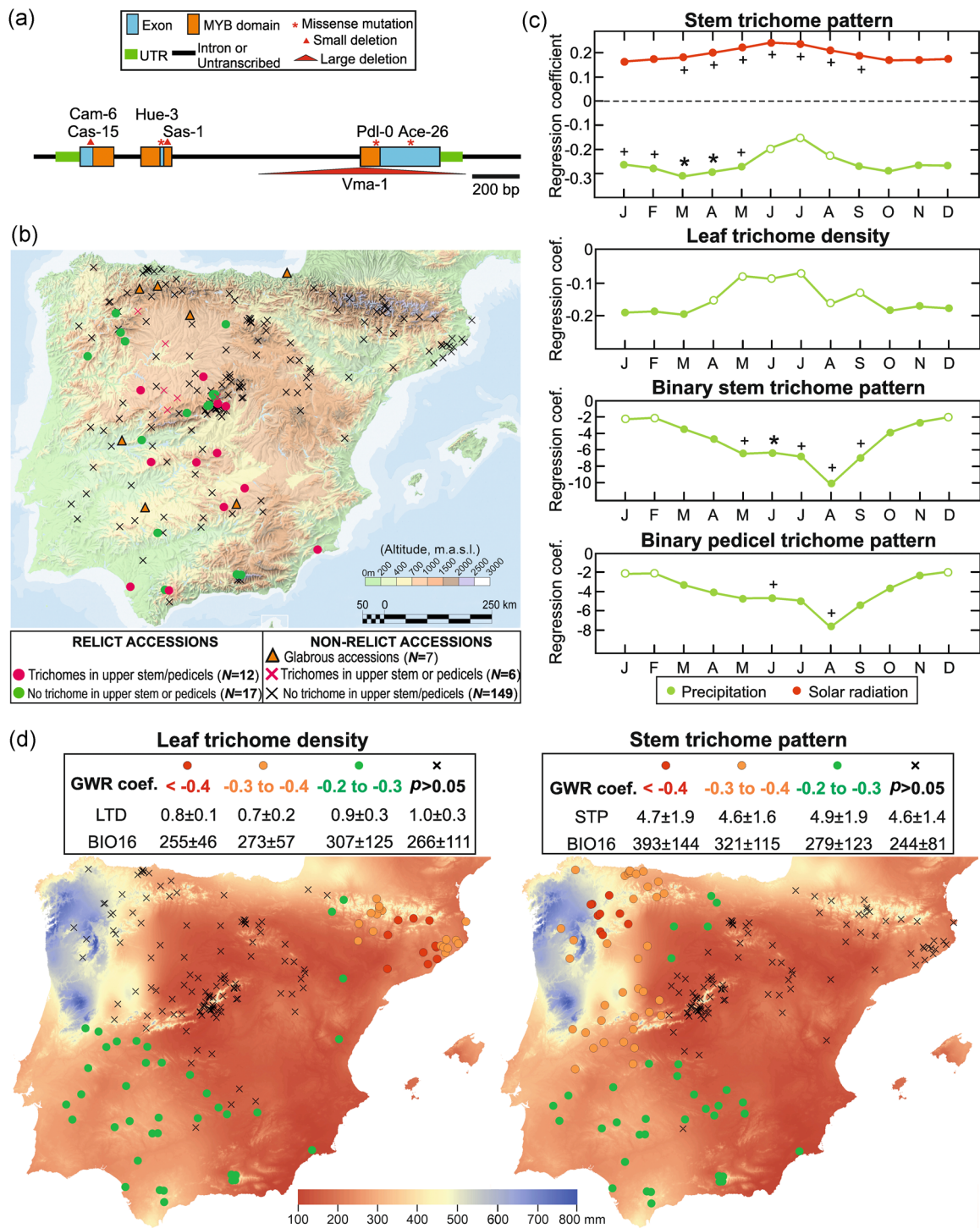


FIGURE 2 Geographic and climatic distribution of trichome patterns in Arabidopsis. (a) *GL1* loss-of-function mutations causing glabrousness in the Iberian Peninsula. (b) Geographic distribution of Iberian populations classified according to qualitative trichome pattern traits (glabrousness, or development of trichomes in fruiting stem internodes and pedicels), and their genetic group (relicts and non-relicts). The number of accessions in each class is indicated in the legend. (c) Relationship between trichome pattern in different organs and monthly precipitation or solar radiation along the year. Months in the abscissa are indicated with the first letter of the month. Filled and white circles depict significant ($p < 0.05$) and nonsignificant ($p > 0.05$) regressions, respectively; plus signs indicate regressions with $p < 0.01$; asterisks point to significant regressions with $p < 0.0006$ (corresponding to 5% with Bonferroni correction for multiple testing). (d) Geographically Weighted Regression (GWR) analyses between precipitation of the wettest quarter (BIO16) and leaf trichome density (left map) or stem trichome pattern (right map). GWR standard coefficients estimated at each location are shown on maps of Iberia BIO16 with different colours according to the upper legend [Color figure can be viewed at wileyonlinelibrary.com]

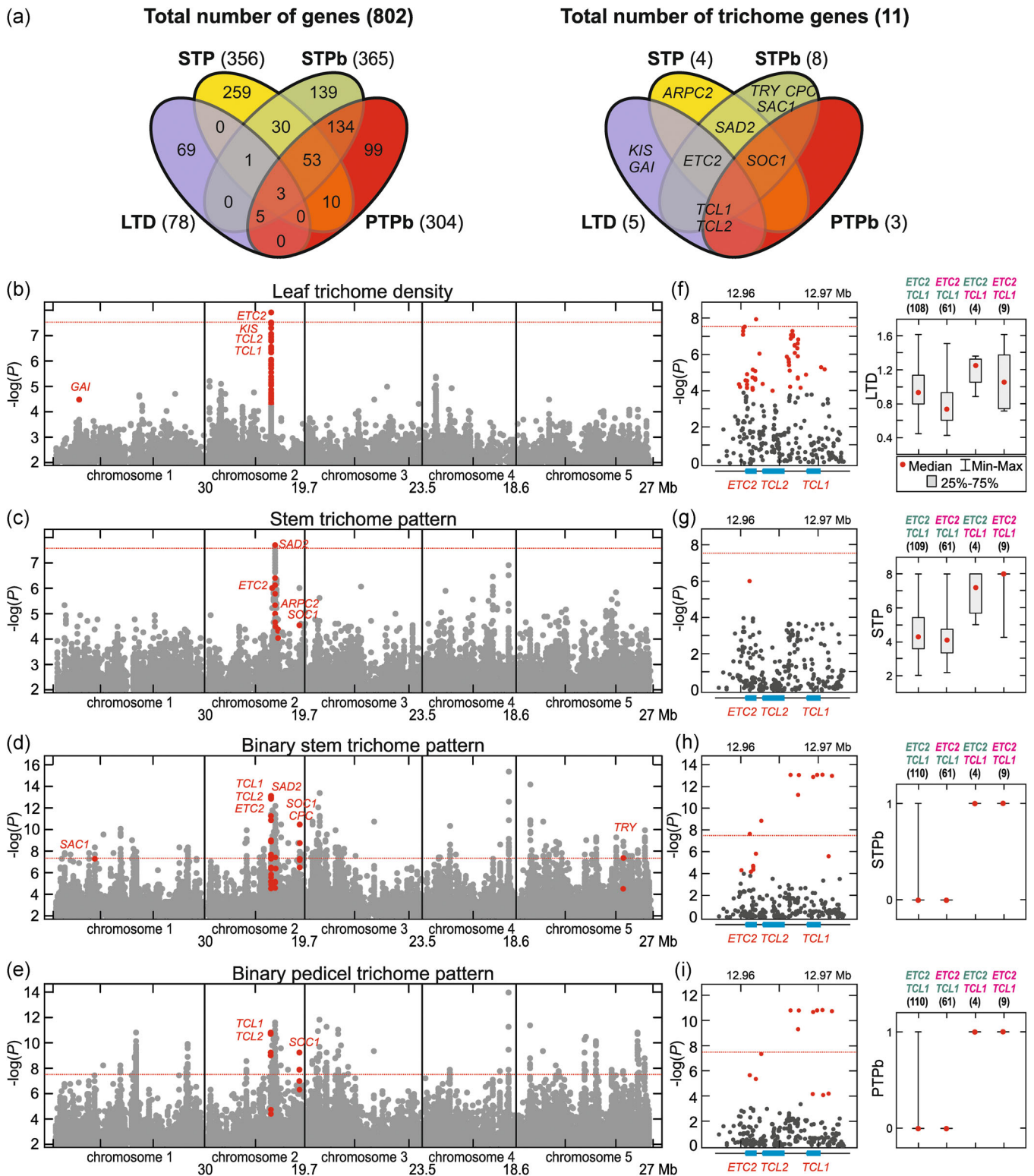


FIGURE 3 (See caption on next page)

TABLE 1 Summary of GWA analyses for trichome pattern traits.

Trait	h^2_b	$h^2_{kinship}$	$h^2_{10\ loci}$	Threshold $-\log(P)^a$	Number of SNPs ^a	Number of genes ^a
LTD	52.8	33.3	62.9	4	178	78
STP	62.8	33.9	57.4	4	650	356
STPb	70.8	72.9	90.0	7	559	365
PTPb	80.0	72.7	80.6	7	792	304

Note: For each trait is shown: the broad-sense heritability (h^2_b); the variance explained by the kinship matrix ($h^2_{kinship}$) or the 10 top associated loci ($h^2_{10\ loci}$); the statistical threshold used for GWA analysis; the number of significant SNPs; and the number of associated genes.

Abbreviations: GWA, genome-wide association; LTD, leaf trichome density; PTPb, binary pedicel trichome pattern; SNP, single nucleotide polymorphism; STP, stem trichome pattern; STPb, binary stem trichome pattern.

^aBinary variables (STPb and PTPb) rendered a larger number of false associations than quantitative traits (LTD, STP), owing to their non-normal and unbalanced phenotypic distributions. To enable comparisons of the genomic regions associated with different traits, a higher statistical threshold was used for binary than quantitative traits.

in trichome development identified significant associations for 11 of them (Figure 3a and Supporting Information: Table S2). These include five of the seven single repeat R3 MYB transcription factors that have been reported to repress trichome formation (Wang & Chen, 2014), two of them (*TRY* and *CPC*) appearing only linked to STPb. Permutation analyses further showed a significant enrichment of such known trichome genes among the associated genes for all traits, but this enrichment was especially strong for LTD (Supporting Information: Figure S2). Together, these results indicate that partly independent genetic bases account for the natural variation in vegetative and reproductive organs.

The most significant genomic region associated with each trait was shared by all organs, and it was located around position 12.9 Mb of chromosome 2 (Figure 3b–e). However, the size of this region was rather small for LTD (< 50 kb), but much larger for STP, STPb and PTPb (~1 Mb) (Supporting Information: Figure S3). This appears then as a complex region that might contain several genes contributing to the natural variation for stem and pedicel trichome patterns (Supporting Information: Table S2). Specially, the gene *SENSITIVE TO ABA AND DROUGHT2* (*SAD2*) involved in trichome initiation

(Gao et al., 2008) showed the strongest association for STP and was detected only for the two stem trichome variables. In addition, the genomic region shared by all four traits included a cluster of three known MYB genes *ETC2*, *TCL1* and *TCL2* that negatively regulate trichome development (Wang & Chen, 2014). Detailed inspection of this cluster showed that the most significant SNPs for leaf trichome patterns were located on *ETC2*, whereas the strongest associations with the binary stem and pedicel trichome patterns appeared on *TCL1* (Figure 3f–i). Since natural mutations in *ETC2* and *TCL1* have been previously demonstrated to affect trichome patterning in leaves and fruits, respectively (Arteaga et al., 2021; Hilscher et al., 2009) we analysed the effect of those polymorphisms (Figure 3f–i). The *ETC2* missense mutation changing Lys¹⁹ to Glu¹⁹ (Hilscher et al., 2009) was segregating at a high similar frequency (38%) in relict and non-relict Iberian accessions (Supporting Information: Table S1). However, the regulatory indel at *TCL1* (Arteaga et al., 2021) showed an overall moderate frequency in this region (7%) and was mostly present in relict accessions (92%). Such *TCL1* polymorphism significantly affected the four trichome traits ($p < 0.002$) as tested by GLMs including both genes as explanatory factors. By contrast, *ETC2* had no effect on stem or pedicel trichome patterns ($p > 0.65$) but showed a marginal effect on LTD ($p = 0.08$) (Figure 3f–i). The allelic effects of both genes were in agreement with previous studies, thus suggesting that *ETC2* and *TCL1* contribute differentially to the natural variation for trichome patterning along plant development.

3.4 | Effect of *TCL1*, *TRY* and *GL1* on trichome patterning

Three of the genes associated with leaf or stem trichome traits, *TCL1*, *TRY* and *GL1*, have been recently shown to be responsible for the diversity for trichome patterning in fruits and pedicels of *Arabidopsis* (Arteaga et al., 2021). These genes underlie the loci *TCL1/MAU2*, *TRY/MAU5* and *GL1/MAU3* previously identified in introgression lines derived from the Iberian accession Don-0, which develops trichomes in fruits, and the laboratory strain Landsberg *erecta* (*Ler*). In addition, Don-0 shows trichomes in pedicels as well as in the upper and lower stem internodes, and it displays higher leaf trichome density than *Ler* (Figures 1c,d and 4a). We then explored the role of these genes on the natural variation for trichome patterning in other organs. To this

FIGURE 3 Genome-wide association analyses of trichome pattern in different organs. (a) Venn diagrams comparing the total number of genes (left side), or the number of known genes involved in trichome development (right side), associated with the four trichome pattern traits (see Table 1). (b–e) Manhattan plots for leaf trichome density (LTD) (b), stem trichome pattern (STP) (c), binary stem trichome pattern (STPb) (d), and binary pedicel trichome pattern (PTPb) (e) across the five *Arabidopsis* chromosomes. (f–i) Zooms of Manhattan plots around the *ETC2/TCL1/TCL2* cluster (left panels) and effect of known polymorphisms of *ETC2* (Hilscher et al., 2009) and *TCL1* (Arteaga et al., 2021) (right panels) on LTD (f), STP (g), STPb (h), and PTPb (i). In (f–i), major and minor alleles of *ETC2* and *TCL1* are coloured in green and magenta, respectively, and the number of accessions for each *ETC2/TCL1* genotypic class is indicated between brackets. In Manhattan plots, a red dotted line indicates the significance threshold of $-\log(P) = 7.53$ (corresponding to 5% with Bonferroni correction for multiple testing). Red coloured dots match single nucleotide polymorphisms located on known trichome related genes that show $-\log(P) > 4$, and the names of these genes are included in each panel [Color figure can be viewed at wileyonlinelibrary.com]

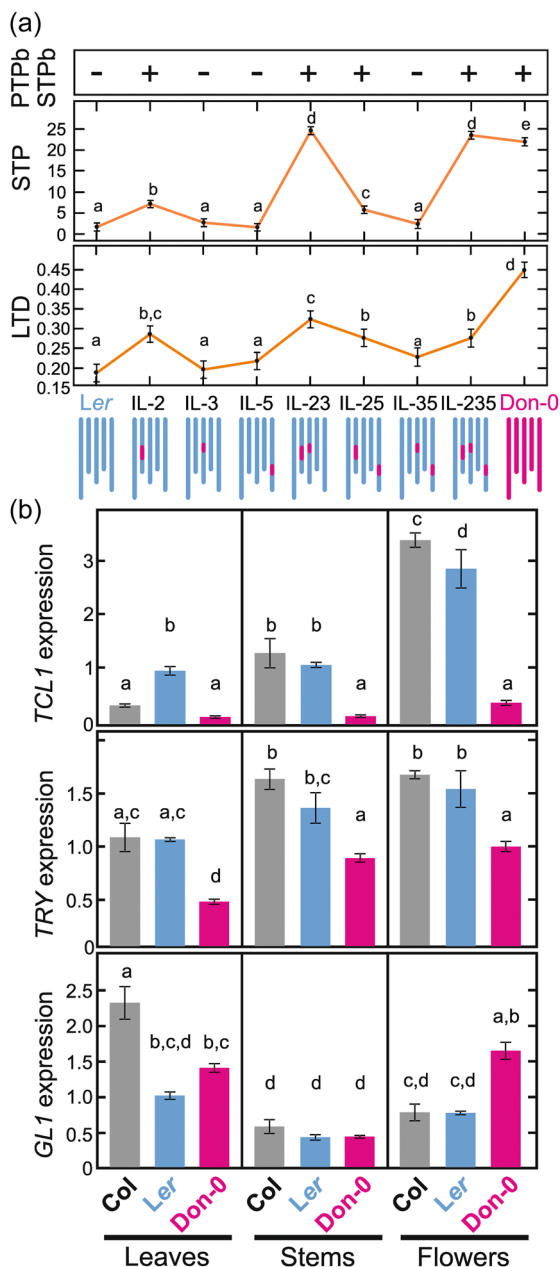


FIGURE 4 Trichome pattern and gene expression of parental and introgression lines. (a) Leaf trichome density (LTD; lower panel), stem trichome pattern (STP; middle panel), as well as the binary trichome patterns in fruiting stems and pedicels (STPb, PTPb; upper panel), of introgression lines differing in Don-0/Ler alleles at *TCL1/MAU2*, *GL1/MAU3* and *TRY/MAU5* genomic regions. For LTD and STP, dots and bars correspond to means \pm 0.95 confidence intervals of three lines per genotype (12–24 plants per line). For STPb and PTPb, “+” and “–” indicate, respectively, the presence and absence of trichomes in the first five fruiting internodes or pedicels. Graphical genotypes of introgression lines (ILs) are depicted in the lower part of the panel. (b) *TCL1*, *TRY* and *GL1* expression in leaves, stems and flower buds of parental accessions. Each bar depicts the mean \pm SE of three biological replicates, and values of all lines are relative to *Ler* vegetative expression. Differences among genotypes for traits or gene expressions were tested by mixed linear models, and the same or different letters indicate non-significant and significant differences, respectively, as measured by Tukey's test ($p < 0.05$) [Color figure can be viewed at wileyonlinelibrary.com]

end, we first measured LTD, STP, PTPb and STPb in seven distinct introgression lines carrying Don-0 alleles in one, two or three genomic regions around these genes, in a *Ler* genetic background (Figure 4a). This analysis shows that the genomic region *TCL1/MAU2* displays a major additive effect on all traits (Figure 4a). Overall, Don-0 alleles in *TCL1/MAU2* increased the amount of trichomes in leaves and stems, explaining 32%–36% of the variance for these traits, and it accounted for the development of trichomes in the upper stem and pedicels (Figure 4a). By contrast, Don-0 alleles at *TRY/MAU5* and *GL1/MAU3* regions only showed small increasing effects on LTD and STP, mostly through genetic interactions with *TCL1/MAU2* region (Supporting Information: Table S3).

A previous study has proven that Don-0 and *Ler* alleles of *TCL1*, *TRY* and *GL1* are functional. However, compared to *Ler*, Don-0 carries partial loss-of-function alleles of the trichome initiation repressors *TCL1* and *TRY*, and a gain-of-function allele of the activator *GL1*, which interact to trigger trichome formation in Don-0 fruits (Arteaga et al., 2021). To elucidate if *TCL1*, *TRY* and *GL1* also cause the variation observed between Don-0 and *Ler* for trichome patterning in leaves and stems, we have further characterized numerous independent transgenic lines homozygous for genomic constructs of these genes from Don-0 and *Ler* (Figure 5 and Supporting Information: Table S3). All transgenes included the promoter, coding and 3'-UTR regions of the parental accessions (see Section 2).

TCL1 transgenes from Don-0 and *Ler* were introduced in the genetic backgrounds of the *tcl1* mutant and the introgression line IL-235. Phenotypic analysis of STP and LTD in 69 transgenic lines revealed significant differences between Don-0 and *Ler* transgenes for both traits in the two backgrounds. Overall, lines carrying *TCL1*-Don-0 transgenes showed a smaller reduction of STP (Figure 5a,d) and LTD (Figure 5b,e) than *TCL1*-*Ler* plants, compared to the untransformed controls. Therefore, the partial loss-of-function allele of the trichome repressor *TCL1* from Don-0 also contributes to the natural variation for LTD and STP. Since *TCL1*-Don-0 allele has been shown to be caused by a deletion in the 3'-UTR (Arteaga et al., 2021), we also analysed transgenic lines for chimeric genomic constructs differing in this gene region. Lines carrying *TCL1* transgenes with 3'-UTR from Don-0 behaved similar to lines with the complete *TCL1*-Don-0 transgene, for STP (Figure 5a,d) and LTD (Figure 5b,e), thus supporting that the 3'-UTR deletion is also the *TCL1* polymorphism that affects these traits. Analysis of *TCL1* expression showed that Don-0 accession has very low expression in leaves, stems and flowers, whereas *Ler* displayed significantly higher expression in flowers than leaves and stems (Figure 4b). Furthermore, comparison of *TCL1* leaf expression between the transgenic lines showed that the 3'-UTR deletion of Don-0 largely reduces the expression (Figure 5c,f and Supporting Information: Table S3). These results, together, indicate that the *cis*-regulatory polymorphism causing hypofunction of *TCL1* in Don-0 accession strongly affects trichome patterning in leaves and stems.

TRY transgenes from Don-0 and *Ler* were introduced in three backgrounds: the *try* mutant and the introgression lines IL-235 and IL-1235 (Figure 5, Supporting Information: Figure S4, Table S3).

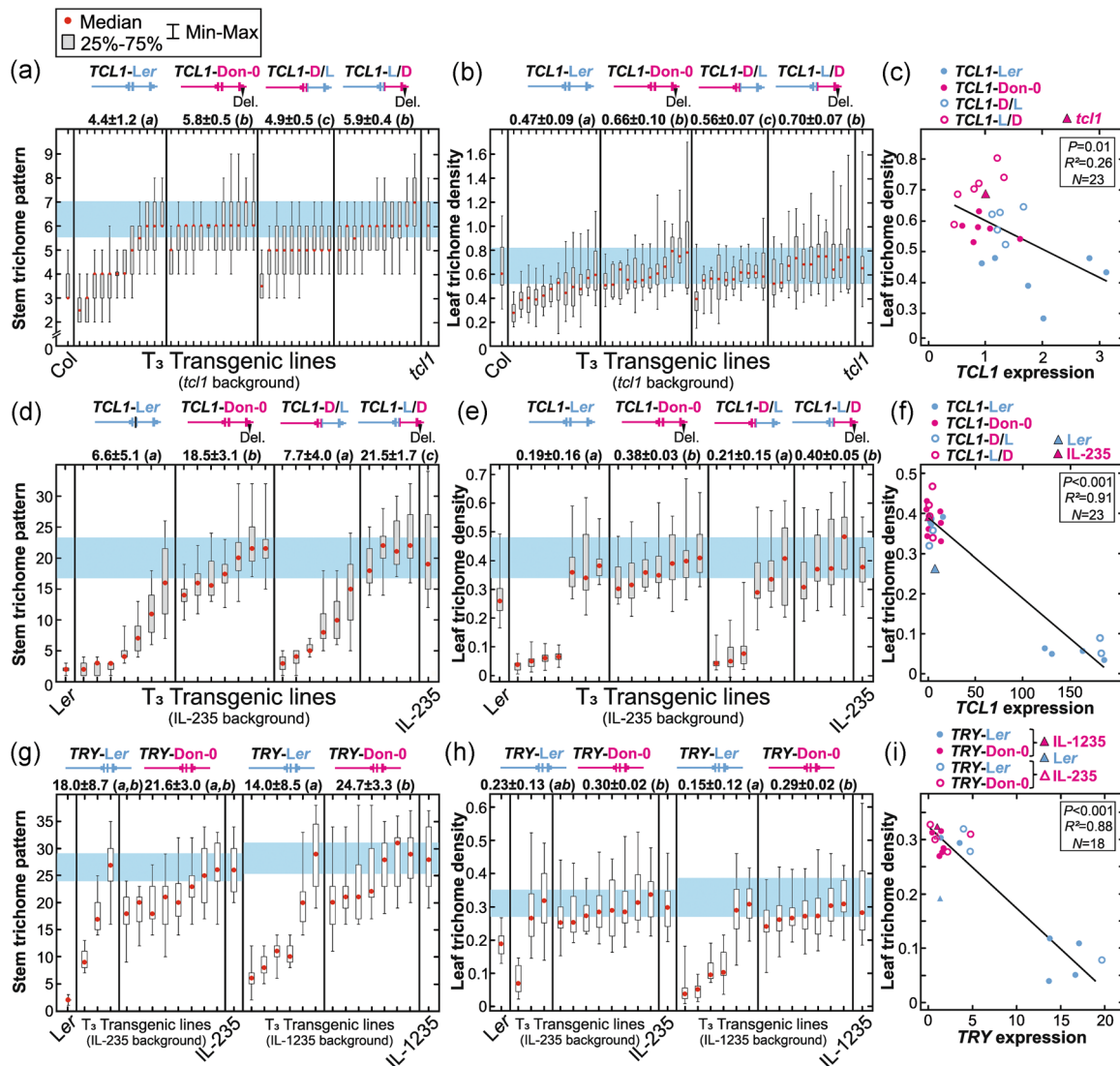


FIGURE 5 Trichome pattern and gene expression of transgenic lines for *TCL1* and *TRY*. (a–e) Stem trichome pattern (a, d), and leaf trichome density (b, e), of independent homozygous transgenic lines carrying parental (left side of panels) or chimeric (right side of panels) genomic constructs of *TCL1*, in *tcl1* mutant (a and b) or IL-235 (d and e) genetic backgrounds. (c and f) Linear regressions between leaf trichome density and *TCL1* expression in leaves, for *TCL1* transgenic lines in *tcl1* (c) or IL-235 (f) backgrounds. (g and h) Stem trichome pattern (g) and leaf trichome density (h) of independent homozygous transgenic lines carrying *Ler* or *Don-0* parental genomic constructs of *TRY* in IL-235 (left side of panels) or IL-1235 (right side of panels) genetic backgrounds. (i) Relationship between leaf trichome density and *TRY* expression in leaves, for *TRY* transgenic lines. Gene expressions of transgenic lines are relative to the expression of untransformed controls. Phenotypic distributions of transgenic lines (derived from 11–18 plants/line) are arranged from low to high mean trait values, and 95% confidence intervals for untransformed controls are shown as blue-shaded areas. The structures of the transgenes are depicted on top of each panel, including the *Don-0* deletion of the 3'-UTR (Del.) described for *TCL1* (Arteaga et al., 2021). Phenotypic differences among genotypes were statistically tested by mixed linear models; the same or different letters on top of each panel indicate non-significant or significant differences, as measured by Tukey's test ($p < 0.05$) [Color figure can be viewed at wileyonlinelibrary.com]

Phenotypic analysis of STP and LTD in 40 transgenic lines showed the differential effect of *Don-0* and *Ler* transgenes depending on the genetic background. In the IL-1235 background, lines bearing *TRY-Don-0* transgenes had smaller reduction of STP and LTD than those with *TRY-Ler* transgenes, compared to the untransformed controls (right panels of Figure 5g,h). Likewise, *TRY* transgenes in *try* background displayed small significant effect on LTD, but not on STP (Supporting Information: Figure S4). On the contrary, transgenic lines

did not differ in any trait in the IL-235 background (left panels of Figure 5g,h). Therefore, the partial loss-of-function allele of the trichome repressor *TRY* described in *Don-0* accession (Arteaga et al., 2021) also contributes to the variation for LTD and STP, but less significantly than *TCL1* and interacting with the genetic background. We further analysed *TRY* expression because the functional alteration of the *TRY-Don-0* allele is caused by regulatory polymorphisms (Arteaga et al., 2021). *Don-0* and *Ler* accessions

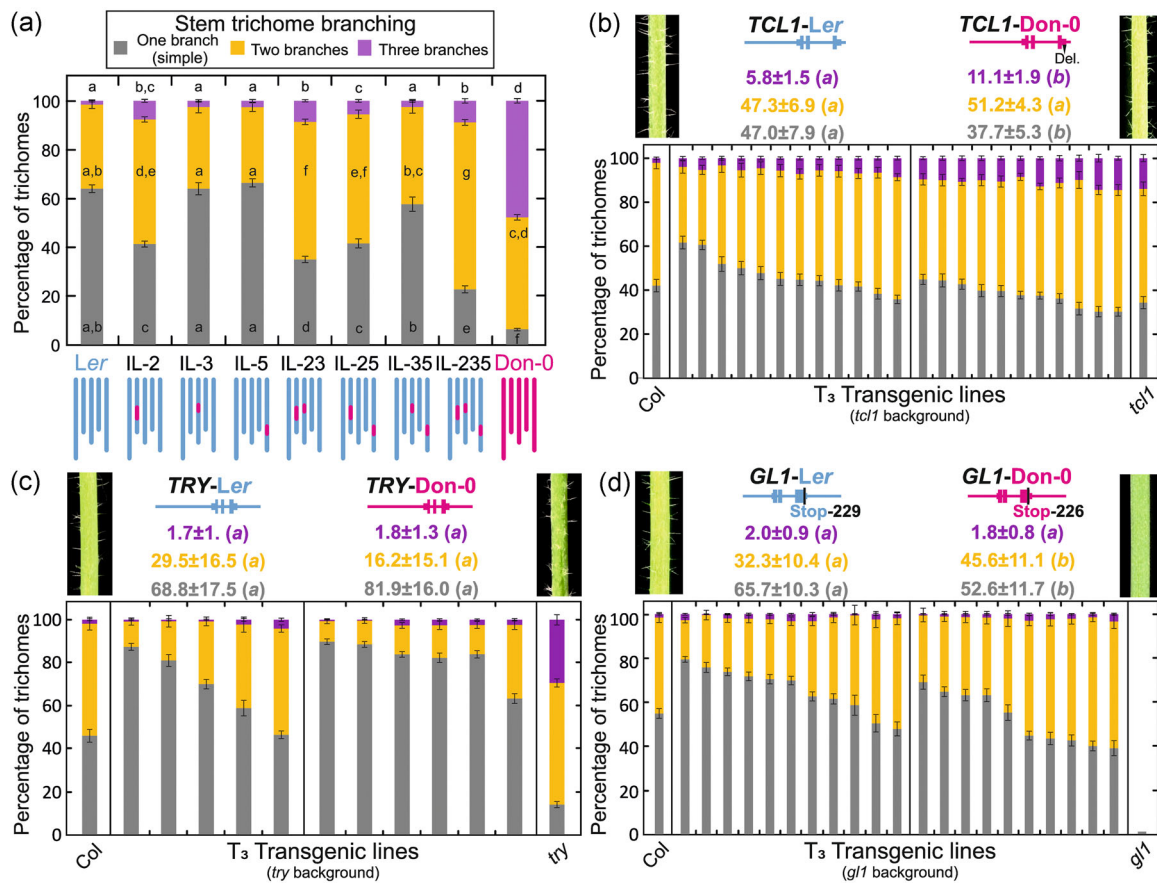


FIGURE 6 Stem trichome branching of mutant, introgression and transgenic lines for *TCL1*, *TRY* and *GL1*. (a) Frequency of stem trichomes with one, two or more than two branches in introgression lines differing in Don-0/Ler alleles at *TCL1/MAU2*, *GL1/MAU3* and *TRY/MAU5* genomic regions. The bar of each genotype shows the percentage \pm SE of trichomes of each branching class quantified in three lines per genotype (8–16 plants per line). (b–d) Frequency of stem trichomes with one, two or more than two branches in independent homozygous transgenic lines carrying Ler or Don-0 genomic constructs of *TCL1* (b), *TRY* (c), or *GL1* (d) in the corresponding mutant genetic background. The bar of each transgenic line shows the percentage \pm SE of trichomes of each branching class quantified in 8–18 plants per line. In (b–d), the average phenotypes of the lines for each transgene, as well as representative stems of mutant lines, are shown on top of each panel. The structures of the transgenes are also depicted on top of the panels, including the main Don-0/Ler polymorphisms described for *TCL1* (deletion of 3'-UTR) and *GL1* (nonsense mutation generating a premature stop codon) (Arteaga et al., 2021). Phenotypic differences among introgression lines or transgenes were statistically tested by mixed linear models; the same or different letters in bars (a), or on top of each panel (b–d) indicate non-significant or significant differences, as tested by Tukey's test ($p < 0.05$) [Color figure can be viewed at wileyonlinelibrary.com]

displayed higher expression in flowers and stems than in leaves. However, Don-0 presented significantly lower expression than Ler in all organs (Figure 4b). Analysis of *TRY* expression in transgenic lines of IL-235 and IL-1235 backgrounds again showed lower leaf expression of *TRY*-Don-0 transgenes compared to *TRY*-Ler (Figure 5i and Supporting Information: Table S3), although statistical differences were only marginal in *try* background (Supporting Information: Figure S4c). Hence, *cis*-regulatory polymorphisms reducing the expression of *TRY*-Don-0 allele also affect STP and LTD.

Finally, characterization of 25 transgenic lines carrying *GL1* alleles from Don-0 and Ler in the *gl1* mutant background did not detect significant differences between Don-0 and Ler transgenes for either STP or LTD (Supporting Information: Figure S4d and S4e). Moreover, we did not find differences in leaf *GL1* expression between Don-0 and Ler transgenes (Supporting Information: Figure S4f and Table S3), in agreement with the pattern of expression

observed in Don-0 and Ler accessions (Figure 4b). Nevertheless, substantial variation was found for *GL1* expression among lines with the same transgene, which correlated with LTD phenotypes, thus suggesting transgene positional effects (Supporting Information: Figure S4f). Therefore, Don-0 gain-of-function allele of the trichome activator *GL1*, previously characterized by a premature stop codon (Arteaga et al., 2021), shows no effect on LTD and STP in *gl1* background.

3.5 | Effect of *TCL1*, *TRY* and *GL1* on trichome branching

We further explored the relevance of these genes on the natural variation for trichome morphology because Don-0 and Ler accessions also differ substantially in the proportion of stem trichomes with

different number of branches (Figure 1d). Overall, most trichomes in Don-0 stems (47.8 ± 4.0) had three or more branches, whereas more than 95% of *Ler* stem trichomes developed only one (simple) or two (Figure 6a). Phenotypic analysis of the introgression lines carrying Don-0 alleles in *TCL1*, *TRY* and/or *GL1* genomic segments showed that *TCL1* region explains 36%–52% of the variation for the proportion of stem trichomes with one, two or three branches (Figure 6a and Supporting Information: Table S3). By contrast, *GL1* and *TRY* regions had small (2%–4%) or nearly absent effects on branching traits, respectively. These results suggest that *TCL1* and *GL1*, but not *TRY*, contribute to Don-0/*Ler* variation for trichome branching. Moreover, the significantly larger proportion of highly branched trichomes of Don-0 indicates that other loci also affect these traits in these accessions.

To validate the role of Don-0/*Ler* allelic variation at *TCL1*, *TRY* and *GL1* genes on trichome branching, we quantified stem branching traits in the transgenic lines described above in the *tcl1*, *try* and *gl1* mutant backgrounds (Figure 6). These analyses showed that lines carrying *TCL1*-Don-0 transgenes developed twice the proportion of trichomes with three branches than lines with *TCL1*-*Ler* transgenes (Figure 6b). Similarly, transgenic lines for *GL1*-Don-0 showed a significant increase on trichomes with two branches (Figure 6d). In agreement with these effects, both *TCL1*-Don-0 and *GL1*-Don-0 transgenes significantly reduced the proportion of simple trichomes. However, lines with *TRY*-Don-0 and *TRY*-*Ler* transgenes did not differ in the proportion of stem trichomes with different number of branches. We concluded that *TCL1* and *GL1*, hence, contribute to the natural variation for trichome branching, the former gene showing a prominent effect.

4 | DISCUSSION

4.1 | Different environmental factors maintain the diversity for trichome patterning across *Arabidopsis* life cycle

Despite the adaptive and taxonomic relevance of the diversity for trichome patterning and morphology in multiple plant organs (Judd et al., 1999), little is known about the underlying genetic, molecular and ecological mechanisms. Our phenotypic characterization shows that *Arabidopsis* contains substantial quantitative intraspecific variation for trichome density in multiple organs beyond leaves (Bloomer et al., 2014; Hilscher et al., 2009). In particular, natural populations also differ in the trichome pattern of stems and fruit pedicels, as well as in the morphology of stem trichomes. Interestingly, several Iberian accessions develop highly branched trichomes in the upper stem internodes carrying flowers, which has not been previously described (Al-Shehbaz & O'Kane, 2002; Yu et al., 2010). These accessions mostly correspond to a set of relict populations that also develop branched trichomes in fruits and pedicels (Arteaga et al., 2021). Thus, novel

trichome patterns in stems, pedicels and fruits have specifically evolved in the ancient relict lineage of Iberia.

Arabidopsis diversity for trichome patterning might be involved in climatic adaptation, as supported by the significant correlations found between trichome traits and precipitation or solar radiation. Overall, the amount of trichomes in all organs increased with low precipitation, but the number of stem internodes developing trichomes also was extended with high solar radiation. These results suggest that *Arabidopsis* variation for trichome patterning is likely involved in adaptation to abiotic (e.g., protection against water loss and UV radiation damage), and/or biotic (e.g., defense against herbivores affected by climate) stresses, as hypothesized for other annual and perennial plants showing similar relationship between trichome density and precipitation (Hahn et al., 2019; Kooyers et al., 2015; Tsujii et al., 2016; Westberg et al., 2013). Furthermore, additional information on the complex interactions between climate and trichome traits is derived from the temporal and spatial variation of climatic factors. First, the specific correlations found between trichomes in leaves, stems or pedicels, and precipitation in the seasons of phenological occurrence of such organs (Exposito-Alonso et al., 2018; Gomaa et al., 2011) suggest a precise fit between trichome patterning and climate throughout the *Arabidopsis* life cycle. Second, GWR analyses show substantial geographic variation for the regressions between trichome traits and precipitation, which indicates that other factors contribute to maintain the variation for these traits in nature. In particular, the spatial variation of the regression coefficients between precipitation and STP suggests that this relationship depends on the particular range of precipitation since the strongest associations are found in the areas with the highest precipitations. By contrast, other local environmental factors seem to contribute to maintain the variation for LTD, because the highest regressions with precipitation appeared in populations with low leaf trichome densities. Furthermore, the six *GL1* loss-of-function mutations described in this study appear as specific to the Iberian region, since none of them has been found in previous worldwide analyses of this gene (Bloomer et al., 2012; Hauser et al., 2001). The very low frequency and geographic distribution of *GL1* loss-of-function mutations reflect the effect of negative natural selection purging such large effect alleles. However, some of those alleles might not be deleterious but maintained by local environmental agents, as suggested by the wider spread of the Iberian Cam-6/Cas-15 *GL1* deletion. Different climatic and local environmental factors, thus, likely contribute to maintain the diversity for trichome patterning in the various organs across the *Arabidopsis* life cycle. Nevertheless, future studies under natural conditions are needed to demonstrate the adaptive processes that might shape trichome pattern diversity. These should address relevant caveats, such as potential trade-offs and pleiotropic relationships between trichome patterning and water use efficiency, herbivore defense or plant growth, as well as the phenotypic plasticity of these traits (McKay et al., 2003; Sobral et al., 2021; Züst & Agrawal, 2017).

4.2 | Differential genomic architectures shape the natural variation for trichome patterning in vegetative and reproductive phases

In agreement with the differential environmental associations detected for trichome traits across the *Arabidopsis* life cycle, GWA analyses show that partly independent genetic bases underlie the diversity for trichome patterning in vegetative and reproductive organs. This is first indicated by the small overlapping (<3%) between the genomic regions associated with LTD and the remaining traits. By contrast, the large overlapping (up to 68%) found between trichome patterning in stems and pedicels indicates shared mechanisms for the variation in multiple organs of the main inflorescence. In particular, we detected 11 previously known genes involved in trichome development, with six of them showing effect only on LTD or STP. These known genes show a significant enrichment among the genes associated with all traits, which suggests that artificial mutagenesis is tagging relevant genes accounting for the natural variation. Specially, the 10-fold higher enrichment found for LTD than for stem or pedicel patterns is in agreement with the larger efforts that have been classically devoted to search for mutants affected in leaf trichomes (Balkunde et al., 2010; Pattanaik et al., 2014).

Five of the seven genes encoding single R3 MYB transcription factors (Wang & Chen, 2014), *TCL1*, *TCL2*, *ETC2*, *TRY* and *CPC*, showed significant associations with one or several traits, indicating that this family of trichome initiation repressors largely contribute to the natural variation for trichome patterning. These genes also show the differential effect on the various traits, because *CPC* and *TRY* were only detected on stem trichome traits, whereas *TCL1* affects the trichomes of all organs. In addition, *ETC2* missense mutation Lys¹⁹/Glu¹⁹ showed the strongest association on leaf trichome density, in agreement with the effect of this polymorphism (Hilscher et al., 2009). Furthermore, the cluster of tandemly repeated genes *ETC2/TCL1/TCL2* illustrates the complex genomic architecture underlying the chromosome 2 GWA locus. These genes correspond to the strongest GWA peak detected on chromosome 2, which was associated with all trichome pattern traits. However, not only the neighbours *TCL1* and *ETC2* affect differentially the various traits, but also the nearby region around the trichome initiation gene *SAD2* (Gao et al., 2008), as suggested by the significant associations found only on stem and pedicel trichome traits. Thus, at least three closely linked genes likely contribute to the natural variation for trichome patterning in different organs of *Arabidopsis*.

Comparison of the genes identified in this regional GWA study with those from previous global GWA analyses also showed a limited overlapping, since only the *ETC2/TCL1/TCL2* cluster and *CPC* genomic regions were common (Atwell et al., 2010). Such small overlapping between studies carried out with regional and global samples can be expected for adaptive traits that are targeted by local or regional environmental factors, as previously described for other traits, such as flowering time (Tabas-Madrid et al., 2018) or gene expression phenotypes (Lopez-Arboleda et al., 2021). This is

supported by the regional geographic variation described above for the relationships between trichomes traits and precipitation. Therefore, additional analyses in other regional or local collections, such as those described for Sweden and France (Brachi et al., 2013; Frachon et al., 2017; Long et al., 2013) will further disentangle the complex interplay between climate and local environmental factors to shape the genetic diversity for trichome patterning across *Arabidopsis* worldwide range.

4.3 | *TCL1*, *TRY* and *GL1* differentially contribute to the natural variation for trichome patterning and branching in multiple organs of *Arabidopsis*

Characterization of introgression and transgenic lines demonstrate that natural variation in the MYB genes *TCL1*, *TRY* and *GL1* account for the diversity not only for trichome patterning in multiple organs but also for the morphology of stem trichomes. Comparisons of the alleles from the relict accession Don-0, developing trichomes in upper stem internodes, pedicels and fruits (this study and Arteaga et al., 2021), and the reference strain Ler, show that *TCL1* strongly affects all traits. By contrast, *TRY* and *GL1* display smaller effects mainly on trichome patterning or branching, respectively.

In agreement with GWA results, the *TCL1*-Don-0 allele showed large additive effects on the pattern of leaves, stems and pedicels. In addition, it also increases the proportion of trichomes with high branching in basal stem internodes, as previously described for *tcl1* loss-of-function mutant alleles (Figure 6b; Tian et al., 2017). Hence, the *cis*-regulatory 3'-UTR deletion reducing the expression and function of *TCL1*-Don allele (Arteaga et al., 2021), pleiotropically increases the amount of trichomes throughout plant development, as well as their branching.

TRY-Don-0 allele also increases trichome density in leaves and stems but depending on the genetic background, which was in concordance with *TRY* detection in GWA analyses only on STPb, and with the extensive genetic interactions previously reported (Doroshkov et al., 2019; Ó'Maoiléidigh et al., 2013; Pesch et al., 2014; Schnittger et al., 1998). In contrast to the increasing effect of the null *try* mutant allele on trichome branching (Figure 6c; Folkers et al., 1997; Perazza et al., 1999), the partial loss-of-function of *TRY*-Don-0 allele showed similar reducing effect than *TRY*-Ler allele on this trait. This result indicates that the low expression of *TRY*-Don-0 is sufficient to repress branching in trichome cells. On the contrary, the gain-of-function of *GL1*-Don-0 allele increases trichome branching, but mainly in the transition from simple to two-branched trichomes, in agreement with previous weak effects described for artificial *GL1* perturbations (Kirik et al., 2005; Marks, 1997). Despite *GL1*-Don-0 allele has been shown to increase trichome density in fruits (Arteaga et al., 2021), we could not detect effects of this allele on trichome patterning in leaves or stems, probably due to *GL1* interactions with *TCL1*, *TRY* (Figure 4a) and other components of this regulatory network (Arteaga et al., 2021; Doroshkov et al., 2019; Pesch et al., 2014; Schnittger et al., 1998). Don-0 alleles thus illustrate

the functional potential of natural variants to modulate the pleiotropy of these genes on trichome patterning and branching.

The natural alleles of the MYB genes *TCL1*, *TRY* and *GL1* described in this study have evolved exclusively in the relict lineage of *Arabidopsis*, widely distributed across Iberia (Figure 2a; Arteaga et al., 2021). These alleles cause a hairy and trichome-branched phenotype in vegetative and reproductive organs, which is presumably involved in climatic adaptation. In addition, other MYB genes, such as *ETC2* and *CPC* (this study; Atwell et al., 2010; Hilscher et al., 2009), as well as different components of the genetic network regulating trichome initiation and branching across the plant life cycle, account for the large *Arabidopsis* diversity for these traits in multiple organs (Bloomer et al., 2014; Symonds et al., 2011). Specially, the functional differentiation of the R3 MYB genes showing distinct expression and/or effect in different organs and accessions (Figure 4b; Arteaga et al., 2021; Kirik et al., 2005; Wang & Chen, 2014) is likely to enable a precise adaptation of trichome traits to different environments across *Arabidopsis* life cycle. Given the adaptive relevance of trichome formation and its environmental plasticity (Hauser, 2014; Holeski et al., 2010; Ogran et al., 2020; Sobral et al., 2021), it can be expected that similar large trichome diversity will also occur in numerous plant species with broad geographic and ecological distributions (Hauser, 2014; Kang et al., 2015; Hahn et al., 2019). The functional conservation of MYB genes on trichome patterning has been recently shown in several species (Vendramin et al., 2014; Yang et al., 2018; reviewed in Chalvin et al., 2020; Fambrini & Pugliesi, 2019; Schuurink & Tissier, 2020; Wang, Yang, et al., 2019). In addition, *GL1* has been shown to be a hotspot for repeated (parallel) evolution of glabrous phenotypes caused by null mutations in the Brassicaceae family (Bloomer et al., 2012; Hauser et al., 2001; Kivimäki et al., 2007; Li et al., 2013; Martin & Orgogozo, 2013). Future studies will further figure out the convergence of mechanisms shaping the natural diversity and adaptation of trichome traits in other Angiosperm plants.

ACKNOWLEDGEMENTS

Authors thank Mercedes Ramiro for technical assistance, and Fabrice Roux for kindly providing the R script for gene enrichment calculations. A.F.-P. and A.M.-S. were recipients of PhD fellowships BES-2017-080063 and PRE2020-094891, respectively, from the Ministerio de Ciencia e Innovación (MCIN) of Spain. This study has been funded by grant PID2019-104249GB-I00 from the MCIN/AEI/10.13039/501100011033 to C.A.-B.

CONFLICTS OF INTEREST

The authors declare no conflicts of interest.

DATA AVAILABILITY STATEMENT

The data that supports the findings of this study are available in the supplementary material of this article.

ORCID

Noelia Arteaga  <http://orcid.org/0000-0001-9951-130X>

Belén Méndez-Vigo  <http://orcid.org/0000-0002-9850-536X>

Alberto Fuster-Pons  <http://orcid.org/0000-0002-9248-4377>

Marija Savic  <http://orcid.org/0000-0003-1588-7655>

Alba Murillo-Sánchez  <http://orcid.org/0000-0001-6441-5297>

F. Xavier Picó  <http://orcid.org/0000-0003-2849-4922>

Carlos Alonso-Blanco  <http://orcid.org/0000-0002-4738-5556>

REFERENCES

- 1001 Genomes Consortium. (2016) 1,135 genomes reveal the global pattern of polymorphism in *Arabidopsis thaliana*. *Cell*, 166, 481–491.
- Aguilar-Jaramillo, A.E., Marin-Gonzalez, E., Matias-Hernandez, L., Osnato, M., Pelaz, S. & Suarez-Lopez, P. (2019) *TEMPRANILLO* is a direct repressor of the microRNA miR172. *Plant Journal*, 100, 522–535.
- Al-Shehbaz, I. & O'Kane, S.L. (2002) Taxonomy and phylogeny of *Arabidopsis* (Brassicaceae). *The Arabidopsis Book*, <https://doi.org/10.1199/tab.0001>
- Arteaga, N., Savic, M., Méndez-Vigo, B., Fuster-Pons, A., Torres-Pérez, R., Oliveros, J.C. et al. (2021) MYB transcription factors drive evolutionary innovations in *Arabidopsis* fruit trichome patterning. *The Plant Cell*, 33, 548–565.
- Atwell, S., Huang, Y.S., Vilhjálmsson, B.J., Willems, G., Horton, M., Li, Y. et al. (2010) Genome-wide association study of 107 phenotypes in *Arabidopsis thaliana* inbred lines. *Nature*, 465, 627–631.
- Balkunde, R., Pesch, M. & Hülskamp, M. (2010) Trichome patterning in *Arabidopsis thaliana* from genetic to molecular models. *Current Topics in Developmental Biology*, 91, 299–321.
- Beale, C.M., Lennon, J.J., Yearsley, J.M., Brewer, M.J. & Elston, D.A. (2010) Regression analysis of spatial data. *Ecology Letters*, 13, 246–264.
- Bickford, C.P. (2016) Ecophysiology of leaf trichomes. *Functional Plant Biology*, 43, 807–814. Available from: <https://doi.org/10.1071/FP16095>
- Bloomer, R.H., Juenger, T.E. & Symonds, V.V. (2012) Natural variation in *GL1* and its effects on trichome density in *Arabidopsis thaliana*. *Molecular Ecology*, 21, 3501–3515.
- Bloomer, R.H., Lloyd, A.M. & Symonds, V.V. (2014) The genetic architecture of constitutive and induced trichome density in two new recombinant inbred line populations of *Arabidopsis thaliana*: phenotypic plasticity, epistasis, and bidirectional leaf damage response. *BMC Plant Biology*, 14, 119.
- Brachi, B., Faure, N., Horton, M., Flahauw, E., Vazquez, A., Nordborg, M. et al. (2010) Linkage and association mapping of *Arabidopsis thaliana* flowering time in nature. *PLOS Genetics*, 6, e1000940.
- Brachi, B., Villoutreix, R., Faure, N., Hautekèete, N., Piquot, Y., Pauwels, M. et al. (2013) Investigation of the geographical scale of adaptive phenological variation and its underlying genetics in *Arabidopsis thaliana*. *Molecular Ecology*, 22, 4222–4240.
- Bradbury, P.J., Zhang, Z., Kroon, D.E., Casstevens, T.M., Ramdoss, Y. & Buckler, E.S. (2007) TASSEL: software for association mapping of complex traits in diverse samples. *Bioinformatics*, 23, 2633–2635.
- Castilla, A.R., Méndez-Vigo, B., Marcer, A., Martínez-Minaya, J., Conesa, D., Picó, F.X. et al. (2020) Ecological, genetic and evolutionary drivers of regional genetic differentiation in *Arabidopsis thaliana*. *BMC Evolutionary Biology*, 20, 71.
- Chalvin, C., Drevensek, S., Dron, M., Bendahmane, A. & Boualem, A. (2020) Genetic control of glandular trichome development. *Trends in Plant Science*, 25, 477–487.
- Dai, X., Wang, G., Yang, D.S., Tang, Y., Broun, P., Marks, M.D. et al. (2010) TrichOME: a comparative omics database for plant trichomes. *Plant Physiology*, 152, 44–54.

- Dalin, P., Agren, J., Bjorkman, C., Huttunen, P. & Karkkainen, K. (2008) Leaf trichome formation and plant resistance to herbivory. In Schaller A. (Ed.) *Induced plant resistance* pp. 89–106. Stuttgart, Germany: Springer.
- Dormann, C. (2007) Assessing the validity of autologistic regression. *Ecological Modelling*, 207, 234–242.
- Doroshkov, A.V., Konstantinov, D.K., Afonnikov, D.A. & Gunbin, K.V. (2019) The evolution of gene regulatory networks controlling *Arabidopsis thaliana* L. trichome development. *BMC Plant Biology*, 19, 53.
- Durvasula, A., Fulgione, A., Gutaker, R.M., Alacakaptan, S.I., Flood, P.J., Neto, C. et al. (2017) African genomes illuminate the early history and transition to selfing in *Arabidopsis thaliana*. *Proceedings of the National Academy of Sciences of the United States of America*, 114, 5213–5218.
- Exposito-Alonso, M., Brennan, A.C., Alonso-Blanco, C. & Pico, F.X. (2018) Spatio-temporal variation in fitness responses to contrasting environments in *Arabidopsis thaliana*. *Evolution*, 72, 1570–1586.
- Fambrini, M. & Pugliesi, C. (2019) The dynamic genetic-hormonal regulatory network controlling the trichome development in leaves. *Plants*, 8, 253.
- Folkers, U., Berger, J. & Hülskamp, M. (1997) Cell morphogenesis of trichomes in *Arabidopsis*: differential control of primary and secondary branching by branch initiation regulators and cell growth. *Development*, 124, 3779–3786.
- Frachon, L., Libourel, C., Villoutreix, R., Carrère, S., Glorieux, C., Huard-Chauveau, C. et al. (2017) Intermediate degrees of synergistic pleiotropy drive adaptive evolution in ecological time. *Nature Ecology and Evolution*, 1, 1551–1561.
- Fürstenberg-Hägg, J., Zagrobelny, M. & Bak, S. (2013) Plant defense against insect herbivores. *International Journal of Molecular Science*, 14, 10242–10297.
- Gao, Y., Gong, X., Cao, W., Zhao, J., Fu, L., Wang, X. et al. (2008) *SAD2* in *Arabidopsis* functions in trichome initiation through mediating *GL3* function and regulating *GL1*, *TTG1* and *GL2* expression. *Journal of Integrative Plant Biology*, 50, 906–917.
- Gomaa, N.H., Montesinos-Navarro, A., Alonso-Blanco, C. & Pico, F.X. (2011) Temporal variation in genetic diversity and effective population size of Mediterranean and subalpine *Arabidopsis thaliana* populations. *Molecular Ecology*, 20, 3540–3554.
- Hahn, P.G., Agrawal, A.A., Sussman, K.I. & Maron, J.L. (2019) Population variation, environmental gradients, and the evolutionary ecology of plant defense against herbivory. *The American Naturalist*, 193, 20–34.
- Hauser, M.T. (2014) Molecular basis of natural variation and environmental control of trichome patterning. *Frontiers in Plant Science*, 5, 320.
- Hauser, M.T., Harr, B. & Schlotterer, C. (2001) Trichome distribution in *Arabidopsis thaliana* and its close relative *Arabidopsis lyrata*: molecular analysis of the candidate gene *GLABROUS1*. *Molecular Biology and Evolution*, 18, 1754–1763.
- Hijmans, R.J., Cameron, S.E., Parra, J.L., Jones, P.G. & Jarvis, A. (2005) Very high resolution interpolated climate surfaces for global land areas. *International Journal of Climatology*, 25, 1965–1978.
- Hilscher, J., Schlotterer, C. & Hauser, M.T. (2009) A single amino acid replacement in *ETC2* shapes trichome patterning in natural *Arabidopsis* populations. *Current Biology*, 19, 1747–1751.
- Holeski, L.M., Chase-Alonge, R. & Kelly, J.K. (2010) The genetics of phenotypic plasticity in plant defense: trichome production in *Mimulus guttatus*. *The American Naturalist*, 175, 391–400.
- Hülskamp, M. & Schnittger, A. (1998) Spatial regulation of trichome formation in *Arabidopsis thaliana*. *Seminars in Cell & Developmental Biology*, 9, 213–220.
- Judd, W.S., Campbell, C.S., Kellogg, E.A. & Stevens, P.F. (1999) *Plant systematics, a phylogenetic approach*. Massachusetts: Sinauer Associates.
- Kang, Y., Sakiroglu, M., Krom, N., Stanton-Geddes, J., Wang, M., Lee, Y.C. et al. (2015) Genome-wide association of drought-related and biomass traits with HapMap SNPs in *Medicago truncatula*. *Plant, Cell & Environment*, 38, 1997–2011.
- Keurentjes, J.J., Bentsink, L., Alonso-Blanco, C., Hanhart, C.J., Blankstijn-De Vries, H., Effgen, S. et al. (2007) Development of a near-isogenic line population of *Arabidopsis thaliana* and comparison of mapping power with a recombinant inbred line population. *Genetics*, 175, 891–905.
- Kirik, V., Lee, M.M., Wester, K., Herrmann, U., Zheng, Z., Oppenheimer, D. et al. (2005) Functional diversification of *MYB23* and *GL1* genes in trichome morphogenesis and initiation. *Development*, 132, 1477–1485.
- Kissling, W.D. & Carl, G. (2008) Spatial autocorrelation and the selection of simultaneous autoregressive models. *Global Ecology and Biogeography*, 17, 59–71.
- Kivimäki, M., Karkkainen, K., Gaudeul, M., Loe, G. & Agren, J. (2007) Gene, phenotype and function: *GLABROUS1* and resistance to herbivory in natural populations of *Arabidopsis lyrata*. *Molecular Ecology*, 16, 453–462.
- Kooyers, N.J., Greenlee, A.B., Colicchio, J.M., Oh, M. & Blackman, B.K. (2015) Replicate altitudinal clines reveal that evolutionary flexibility underlies adaptation to drought stress in annual *Mimulus guttatus*. *The New Phytologist*, 206, 152–165.
- Li, F., Zou, Z., Yong, H.Y., Kitashiba, H. & Nishio, T. (2013) Nucleotide sequence variation of *GLABRA1* contributing to phenotypic variation of leaf hairiness in Brassicaceae vegetables. *Theoretical and Applied Genetics*, 126, 1227–1236.
- Liu, X., Bartholomew, E., Cai, Y. & Ren, H. (2016) Trichome-related mutants provide a new perspective on multicellular trichome initiation and development in Cucumber (*Cucumis sativus* L.). *Frontiers in Plant Science*, 7, 1187.
- Long, Q., Rabanal, F.A., Meng, D., Huber, C.D., Farlow, A., Platzer, A. et al. (2013) Massive genomic variation and strong selection in *Arabidopsis thaliana* lines from Sweden. *Nature Genetics*, 45, 884–890.
- Lopez-Arboleda, W.A., Reinert, S., Nordborg, M. & Korte, A. (2021) Global genetic heterogeneity in adaptive traits. *Molecular Biology and Evolution*, 38, 4822–4831.
- Manzano-Piedras, E., Marcer, A., Alonso-Blanco, C. & Pico, F.X. (2014) Deciphering the adjustment between environment and life history in annuals: lessons from a geographically-explicit approach in *Arabidopsis thaliana*. *PLOS One*, 9, e87836.
- Marks, M.D. (1997) Molecular genetic analysis of trichome development in *Arabidopsis*. *Annual Review of Plant Physiology and Plant Molecular Biology*, 48, 137–163.
- Martin, A. & Orgogozo, V. (2013) The loci of repeated evolution: a catalog of genetic hotspots of phenotypic variation. *Evolution*, 67, 1235–1250.
- McKay, J.K., Richards, J.H. & Mitchell-Olds, T. (2003) Genetics of drought adaptation in *Arabidopsis thaliana*: I. Pleiotropy contributes to genetic correlations among ecological traits. *Molecular Ecology*, 12, 1137–1151.
- Mediavilla, S., Martin, I., Babiano, J. & Escudero, A. (2019) Foliar plasticity related to gradients of heat and drought stress across crown orientations in three Mediterranean *Quercus* species. *PLOS One*, 14, e0224462.
- Ó'Maoléidigh, D.S., Wuest, S.E., Rae, L., Raganelli, A., Ryan, P.T., Kwaśniewska, K. et al. (2013) Control of reproductive floral organ identity specification in *Arabidopsis* by the C function regulator *AGAMOUS*. *The Plant Cell*, 25, 2482–2503.
- Ogran, A., Conner, J., Agrawal, A.A. & Barazani, O. (2020) Evolution of phenotypic plasticity: genetic differentiation and additive genetic variation for induced plant defence in wild arugula *Eruca sativa*. *Journal of Evolutionary Biology*, 33, 237–246.

- Pattanaik, S., Patra, B., Singh, S.K. & Yuan, L. (2014) An overview of the gene regulatory network controlling trichome development in the model plant, *Arabidopsis*. *Frontiers in Plant Science*, 5, 259.
- Perazza, D., Herzog, M., Hülkamp, M., Brown, S., Dorne, A.M. & Bonneville, J.M. (1999) Trichome cell growth in *Arabidopsis thaliana* can be derepressed by mutations in at least five genes. *Genetics*, 152, 461–476.
- Pesch, M., Dartan, B., Birkenbihl, R., Somssich, I.E. & Hülkamp, M. (2014) *Arabidopsis* TTG2 regulates TRY expression through enhancement of activator complex-triggered activation. *The Plant Cell*, 26, 4067–4083.
- Rangel, T.F., Diniz-Filho, J.A.F. & Bini, L.M. (2010) SAM: a comprehensive application for spatial analysis in macroecology. *Ecography*, 33, 46–50.
- Rosenberg, M.S. & Anderson, C.D. (2011) PASSaGE: pattern analysis, spatial statistics and geographic exegesis. version 2. *Methods in Ecology and Evolution*, 2, 229–232.
- Schellmann, S., Schnittger, A., Kirik, V., Wada, T., Okada, K., Beermann, A. et al. (2002) TRIPTYCHON and CAPRICE mediate lateral inhibition during trichome and root hair patterning in *Arabidopsis*. *The EMBO Journal*, 21, 5036–5046.
- Schnittger, A., Jurgens, G. & Hülkamp, M. (1998) Tissue layer and organ specificity of trichome formation are regulated by GLABRA1 and TRIPTYCHON in *Arabidopsis*. *Development*, 125, 2283–2289.
- Schuurink, R. & Tissier, A. (2020) Glandular trichomes: micro-organs with model status? *The New Phytologist*, 225, 2251–2266.
- Sobral, M., Sampedro, L., Neylan, I., Siemens, D. & Dirzo, R. (2021) Phenotypic plasticity in plant defense across life stages: inducibility, transgenerational induction, and transgenerational priming in wild radish. *Proceedings of the National Academy of Sciences of the United States of America*, 118, e2005865118.
- Sun, L., Zhang, A., Zhou, Z., Zhao, Y., Yan, A., Bao, S. et al. (2015) GLABROUS INFLORESCENCE STEMS3 (GIS3) regulates trichome initiation and development in *Arabidopsis*. *The New Phytologist*, 206, 220–230.
- Symonds, V.V., Hatlestad, G. & Lloyd, A.M. (2011) Natural allelic variation defines a role for ATMYC1: trichome cell fate determination. *PLOS Genetics*, 7, e1002069.
- Tabas-Madrid, D., Méndez-Vigo, B., Arteaga, N., Marcer, A., Pascual-Montano, A., Weigel, D. et al. (2018) Genome-wide signatures of flowering adaptation to climate temperature: regional analyses in a highly diverse native range of *Arabidopsis thaliana*. *Plant, Cell & Environment*, 41, 1806–1820.
- Tan, Y., Barnbrook, M., Wilson, Y., Molnar, A., Bukys, A. & Hudson, A. (2020) Shared mutations in a novel glutaredoxin repressor of multicellular trichome fate underlie parallel evolution of *Antirrhinum* species. *Current Biology*, 30, 1357–1366.
- Tian, H., Wang, X., Guo, H., Cheng, Y., Hou, C., Chen, J.G. et al. (2017) NTL8 regulates trichome formation in *Arabidopsis* by directly activating R3 MYB genes TRY and TCL1. *Plant Physiology*, 174, 2363–2375.
- Togninalli, M., Seren, Ü., Meng, D., Fitz, J., Nordborg, M., Weigel, D. et al. (2017) The AraGWAS catalog: a curated and standardized *Arabidopsis thaliana* GWAS catalog. *Nucleic Acids Research*, 46, D1150–D1156.
- Tsuji, Y., Onoda, Y., Izuno, A., Isagi, Y. & Kitayama, K. (2016) A quantitative analysis of phenotypic variations of *Metrosideros polymorpha* within and across populations along environmental gradients on Mauna Loa, Hawaii. *Oecologia*, 180, 1049–1059.
- Tutin, T.G., Burges, N.A., Chater, A.O., J.R., E., Heywood, V.H. & Moore, D.M. et al. (1993) *Flora Europaea*. Cambridge University Press.
- Vendramin, E., Pea, G., Dondini, L., Pacheco, I., Dettori, M.T., Gazza, L. et al. (2014) A unique mutation in a MYB gene cosegregates with the nectarine phenotype in peach. *PLOS One*, 9, e90574.
- Wang, S. & Chen, J.G. (2014) Regulation of cell fate determination by single-repeat R3 MYB transcription factors in *Arabidopsis*. *Frontiers in Plant Science*, 5, 133.
- Wang, Z., Yang, Z. & Li, F. (2019) Updates on molecular mechanisms in the development of branched trichome in *Arabidopsis* and nonbranched in cotton. *Plant Biotechnology Journal*, 17, 1706–1722.
- Wang, L., Zhou, C.M., Mai, Y.X., Li, L.Z., Gao, J., Shang, G.D. et al. (2019) A spatiotemporally regulated transcriptional complex underlies heteroblastic development of leaf hairs in *Arabidopsis thaliana*. *EMBO Journal*, 38, e100063.
- Westberg, E., Ohali, S., Shevelevich, A., Fine, P. & Barazani, O. (2013) Environmental effects on molecular and phenotypic variation in populations of *Eruca sativa* across a steep climatic gradient. *Ecology and Evolution*, 3, 2471–2484.
- Yang, S., Cai, Y., Liu, X., Dong, M., Zhang, Y., Chen, S. et al. (2018) A CsMYB6-CSTRY module regulates fruit trichome initiation in cucumber. *Journal of Experimental Botany*, 69, 1887–1902.
- Yu, N., Cai, W.J., Wang, S., Shan, C.M., Wang, L.J. & Chen, X.Y. (2010) Temporal control of trichome distribution by microRNA156-targeted SPL genes in *Arabidopsis thaliana*. *The Plant Cell*, 22, 2322–2335.
- Zhou, L.H., Liu, S.B., Wang, P.F., Lu, T.J., Xu, F., Genin, G.M. et al. (2017) The *Arabidopsis* trichome is an active mechanosensory switch. *Plant, Cell & Environment*, 40, 611–621.
- Züst, T., Heichinger, C., Grossniklaus, U., Harrington, R., Kliebenstein, D.J. & Turnbull, L.A. (2012) Natural enemies drive geographic variation in plant defenses. *Science*, 338, 116–119.
- Züst, T. & Agrawal, A.A. (2017) Trade-offs between plant growth and defense against insect herbivory: An emerging mechanistic synthesis. *Annual Review Plant Biology*, 68, 513–534.

SUPPORTING INFORMATION

Additional supporting information may be found in the online version of the article at the publisher's website.

How to cite this article: Arteaga, N., Méndez-Vigo, B., Fuster-Pons, A., Savic, M., Murillo-Sánchez, A., Picó, F.X., et al. (2022) Differential environmental and genomic architectures shape the natural diversity for trichome patterning and morphology in different *Arabidopsis* organs. *Plant, Cell & Environment*, 45, 3018–3035.
<https://doi.org/10.1111/pce.14308>